

## Octupole and Quadrupole Transition Rates in $F^{19}$ from Scattering of 15-MeV Deuterons\*

D. DEHNHARD AND NORTON M. HINTZ

*Williams Laboratory of Nuclear Physics, University of Minnesota, Minneapolis, Minnesota 55455*

(Received 21 November 1969)

Angular distributions of 15.0-MeV deuterons scattered by  $F^{19}$  were measured between  $\theta_{\text{lab}} = 18^\circ$  and  $85^\circ$ . Inelastic groups leaving  $F^{19}$  in its five lowest-lying excited states were observed using two position-sensitive detectors placed in the focal plane of a split-pole spectrometer. The elastic-scattering cross section was analyzed using an optical model.  $B(E2) \downarrow$  values for the transitions from the  $\frac{5}{2}^+$  (0.197-MeV) and the  $\frac{3}{2}^+$  (1.56-MeV) states to the ground state were found to be  $9 \pm 3$  and  $10 \pm 3$  W.u. (single-particle units). They were calculated from the  $\beta_2$  deformation parameter extracted from a distorted-wave Born-approximation (DWBA) analysis using a complex form factor derived from the optical-model analysis with a surface-absorption term. These results are in good agreement with results obtained from inelastic proton scattering and from Coulomb-excitation experiments. However, the  $B(E3) \downarrow$  value for the  $\frac{5}{2}^- \rightarrow \frac{1}{2}^+$  transition from the 1.35-MeV state was found to be  $1.4 \pm 0.6$  W.u. as compared to the upper limit of  $3.8 \pm 0.6$  W.u. from a  $(p, p')$  experiment, and to  $12.0 \pm 4.0$  and  $7.6 \pm 1.3$  W.u. from two different Coulomb-excitation experiments. The results are compared to various model predictions.

### INTRODUCTION

IN general, multipole transition matrix elements  $B(EL)$  extracted from Coulomb excitation of collective states are found to be in good agreement with the results of a collective-form-factor (CFF) analysis of inelastic scattering experiments.<sup>1</sup>

Recently, a serious discrepancy between a Coulomb excitation experiment and an inelastic proton scattering experiment was found.<sup>2</sup>

Litherland *et al.*<sup>3</sup> investigated the Coulomb excitation of the  $J^\pi = \frac{5}{2}^-$  state of  $F^{19}$  at 1.35 MeV (see Fig. 1) by bombarding various targets with a 18-35-MeV  $F^{19}$  beam. They extracted a  $B(E3) \downarrow$  value of  $12.0 \pm 4.0$  W.u. (Weisskopf units or single-particle units as defined in Ref. 4), a value larger than can be explained by any reasonable model. Crawley and Garvey<sup>2</sup> studied the inelastic scattering of 17.5-MeV protons from  $F^{19}$  and found an upper limit of only  $3.8 \pm 0.6$  W.u. from a CFF analysis with real coupling.

Quite recently, Alexander *et al.*<sup>5</sup> investigated the Coulomb excitation of  $F^{19}$  by bombarding a Si target with a  $F^{19}$  beam at energies between 22 and 28 MeV. Their  $B(E3) \downarrow$  value is  $7.6 \pm 1.3$  W.u. and thus considerably smaller than the previously reported value.

These discrepancies are of interest because considerable effort has been spent trying to explain theoretically the large  $B(E3)$  value originally reported, however with very little success.

We have studied the inelastic scattering of deuterons from  $F^{19}$  to make an independent measurement of this quantity.

Further information on low-lying  $F^{19}$  states was obtained by Lutz *et al.*<sup>6</sup> from a  $(p, p')$  experiment at 13.9 MeV and by Newton *et al.*<sup>7</sup> from a  $(p, p')$  experiment at 140 MeV.

Unlike the  $L=3$  transition to the 1.35-MeV state, the  $L=2$  transitions to the strongly excited states at 0.197 and 1.56 MeV (see Fig. 1) have shown good agreement between Coulomb excitation and inelastic scattering results.

### EXPERIMENTAL PROCEDURE

Targets of about  $20 \mu\text{g}/\text{cm}^2$   $\text{CaF}_2$  were made by evaporation onto a thin ( $10\text{-}\mu\text{g}/\text{cm}^2$ ) carbon backing. A 15.00-MeV deuteron beam from the MP Tandem Van de Graaff of typically 200-500 nA was focused into the scattering chamber of a split-pole spectrograph.<sup>8</sup> A scattering chamber entrance aperture of 1 mm width and 2 mm height limited the target spot size to an area of less than  $1 \times 2 \text{ mm}^2$  and the contribution of the target width to the total image width in the focal plane of the spectrometer to less than 0.3 mm. The spectrometer entrance slits were set 12 mm wide and 7 mm high at a distance of 23 cm from the target thus defining a solid angle of about 1.6 msr.

Two position sensitive detectors, each 500  $\mu$  thick, 30 mm long, and 10 mm high, were placed at the proper kinematical focus of the spectrometer at the high energy end of the focal plane. The distance between the two detectors was chosen so that the two

\* Work supported in part by U.S. Atomic Energy Commission.

<sup>1</sup> W. T. Pinkston and G. R. Satchler, Nucl. Phys. **27**, 270 (1961); see also references in G. R. Satchler, *ibid.* **77**, 481 (1966).

<sup>2</sup> G. M. Crawley and G. T. Garvey, Phys. Rev. **167**, 1070 (1968).

<sup>3</sup> A. E. Litherland, M. A. Clark, and C. Broude, Phys. Letters **3**, 204 (1963).

<sup>4</sup> S. J. Skorka, J. Hertel, and T. W. Retz-Schmidt, Nucl. Data **2**, 347 (1966).

<sup>5</sup> T. K. Alexander, O. Hausser, K. W. Allen, and A. E. Litherland, Bull. Phys. Soc. **14**, 123 (1969); Can. J. Phys. **47**, 2335 (1969).

<sup>6</sup> H. F. Lutz, J. J. Wesolowski, L. F. Hansen, and S. F. Eccles, Phys. Letters **20**, 410 (1966).

<sup>7</sup> D. Newton, A. B. Legg, and G. L. Salmon, Nucl. Phys. **55**, 353 (1964).

<sup>8</sup> J. E. Spencer and H. A. Enge, Nucl. Instr. Methods **49**, 181 (1967).

triplets (ground state, the 0.110- and 0.197-MeV states, and the 1.35-, 1.46-, and 1.56-MeV states) could be measured simultaneously. Because deuterons of approximately 15 MeV were not stopped in the 500- $\mu$ -thick detector (positioned at  $45^\circ$  to the incident particles), the computer code DIVIDE<sup>9</sup> was used to divide the  $XE$  signal by the  $E$  signal. This cancels the appreciable energy spread present in both, when the particles are not stopped.

Figures 2 and 3 show position spectra obtained from detector 1 at  $\theta_{lab}=45^\circ$  and from detector 2 at  $85^\circ$ .

The peak width was found to be about 7 keV, equivalent to an over-all resolution of  $E/\Delta E=2 \times 10^3$ .

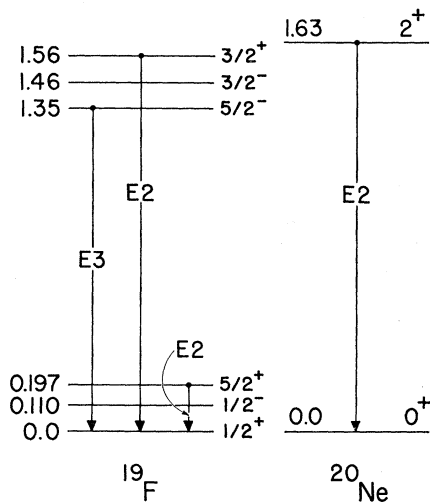


FIG. 1. Level scheme of low-lying states in  $F^{19}$  and  $Ne^{20}$ .

The resolution was limited to this value because of contributions from target thickness, detector noise, target spot size, initial beam energy spread, incoming beam divergence, and spectrometer aberrations, all contributions being of the same order of magnitude.

The 10-mm-high detectors fully covered the approximately 6-mm-high image of the 2-mm-high target spot.

A peak width of only 7 keV is quite useful for resolving the rather weakly excited states at 0.110 and 1.46 MeV. The groups from the elastic scattering from  $O^{16}$  and  $C^{12}$  in Figs. 2 and 3 are considerably wider than the groups from  $F^{19}$  because the focal plane was set for the  $F^{19}(d, d')$  reaction, thus leaving the  $O^{16}(d, d)$  and  $C^{12}(d, d)$  reactions off the kinematic focus. The above illustrates a serious problem connected with this type of spectrometer. When large solid angles are used, the lighter or heavier contaminants may interfere strongly with the groups

<sup>9</sup> P. H. Debenham, D. Dehnhard, and R. W. Goodwin, Nucl. Instr. Methods **67**, 288 (1969).

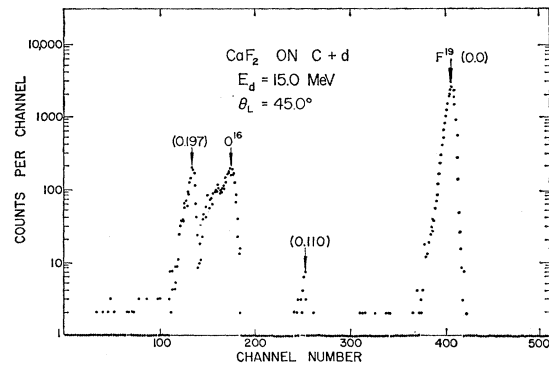


FIG. 2. Position spectrum of detector 1 at  $\theta_{lab}=45^\circ$ .

of interest because the former are detected far from their kinematic focus.

To check for possible alignment errors caused by fringing fields, the yield from elastic scattering was measured at several far forward angles on both sides of the beam. A correction in the scattering angle of  $0.15^\circ$  was found necessary. With this correction the scattering angle was known to better than  $0.1^\circ$ .

#### OPTICAL-MODEL ANALYSIS

Approximate absolute cross sections were obtained by normalizing the yield of the elastic scattering to data obtained by Denes *et al.*<sup>10</sup> at  $15.0 \pm 0.2$  MeV. The agreement of the relative differential cross sections with the latter data is very good (Fig. 4) except at the most forward angle measured by Denes *et al.* ( $\theta_{c.m.}=26.8^\circ$ ). Our data between  $\theta_{c.m.}=19.35^\circ$  and  $\theta_{c.m.}=91.25^\circ$  and Denes's data at larger angles up to  $\theta_{c.m.}=156.8^\circ$  were analyzed by an optical model (Fig. 4). The optical-model search program RAROMP<sup>11</sup> was used applying a potential of the independent Woods-

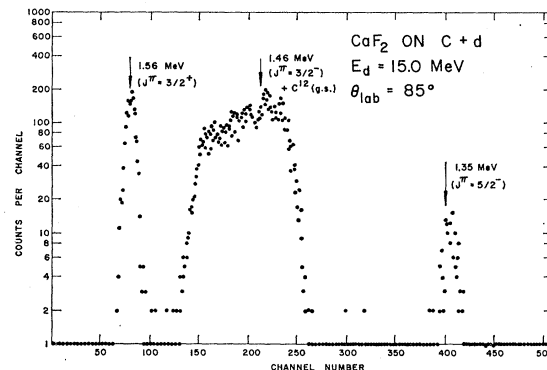


FIG. 3. Position spectrum of detector 2 at  $\theta_{lab}=85^\circ$ .

<sup>10</sup> L. J. Denes, W. W. Daehnick, and R. M. Drisko, Phys. Rev. **148**, 1097 (1966); L. J. Denes, Ph.D. thesis, University of Pittsburgh, 1965 (unpublished).

<sup>11</sup> G. J. Pyle, J. H. Williams Laboratory Internal Report, University of Minnesota (unpublished).

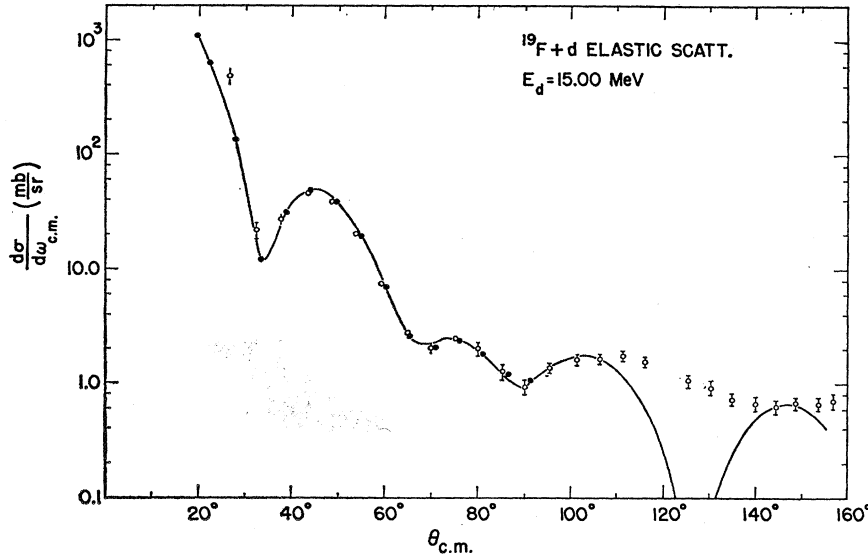


FIG. 4. Differential cross sections of the elastic scattering. Full circles: present experiment; open circles: data of Ref. 10; solid line: optical-model fit with surface absorption.

Saxon form with volume or with surface absorption. Two different searches were performed, one with a pure volume, the other with a pure surface term for the absorption potential. Spin-orbit interaction was not included.

It is generally accepted<sup>12</sup> that the pure surface term of the absorption potential is to be used in the analysis of elastic scattering of deuterons off nuclei. However, the derivative of the optical-model potential is used as a form factor in the distorted-wave analysis of the inelastic scattering. Therefore, it appears likely<sup>13</sup> that the node in the derivative of the surface term may affect the shape and the absolute cross section of the inelastic scattering if compared to calculations with a form factor derived from a volume term. Equally good fits to the elastic scattering were obtained for both shapes of the absorption potential. Because absolute cross sections were not well known, the search was performed with various normalization factors for the elastic-scattering cross section (between 1.0 and 1.3).

The minimum in  $\chi^2$  (as a function of the normalization constant) was found at very closely the same normalization constant for the two searches with volume and with surface absorption. In the latter case the value of the constant was 1.26. The cross sections in the Figs. 4-7 include this factor. We believe that the absolute cross section obtained this way is accurate to better than 20%. The over-all fit to the elastic scattering is good except at backward angles. As was pointed out by Denes *et al.*,<sup>10</sup> this is probably due to the spin-orbit term in the optical-model potential, which we neglected.

When performing the optical-model search we

started with the set of potentials of Ref. 10. The results are given in Table I. Although the depth and radius of the imaginary parts of the potential are quite different for volume and surface absorption, their rms radii were found to be very closely the same.

#### DWBA ANALYSIS; DEFORMATION PARAMETERS $\beta_L$ AND $B(EL)$ TRANSITION PROBABILITIES

Using the computer code DWUCK<sup>14</sup> inelastic differential cross sections were calculated to extract the deformation parameter  $\beta_L$ . In this type of analysis we are assuming the excited states to be collective shape excitations of the nuclear surface (vibrations or rotations). As usual, only the first derivative term of the Taylor expansion of the complex optical potential was used as the form factor. For  $0^+ \rightarrow J^\pi$  transitions with angular momentum transfer  $L=J$  the experimental cross section is related to the calculated cross section  $\sigma_{lsj}(\theta)$  through

$$(d\sigma/d\omega_{0 \rightarrow L})(\text{expt}) = \beta_L^2 \sigma_{lsj}(\theta) \quad (1)$$

when the potential strengths  $V_r$  and  $W_V$  (or  $W_D$ ) are included in the form factor. If the target spin is different from zero, as in the present investigation, the total transition strength will be split among several states. In general, the splitting will be model-dependent.<sup>15</sup> In the strong-coupling rotational model we have

$$(d\sigma/d\omega_{J_i \rightarrow J_f})(\text{expt}) = (J_i L K 0 / J_f K)^2 \beta_L^2 \sigma_{lsj}(\theta), \quad (2)$$

where  $J_i$ ,  $J_f$  are the spins of the initial and final states and  $K$  is their projection number along the nuclear symmetry axis. In the weak-coupling model the rela-

<sup>12</sup> C. M. Perey and F. G. Perey, Phys. Rev. **132**, 755 (1963).

<sup>13</sup> J. K. Dickens, F. G. Perey, and G. R. Satchler, Nucl. Phys. **73**, 529 (1965).

<sup>14</sup> P. D. Kunz (private communication).

<sup>15</sup> K. Alder *et al.*, Rev. Mod. Phys. **28**, 432 (1956).

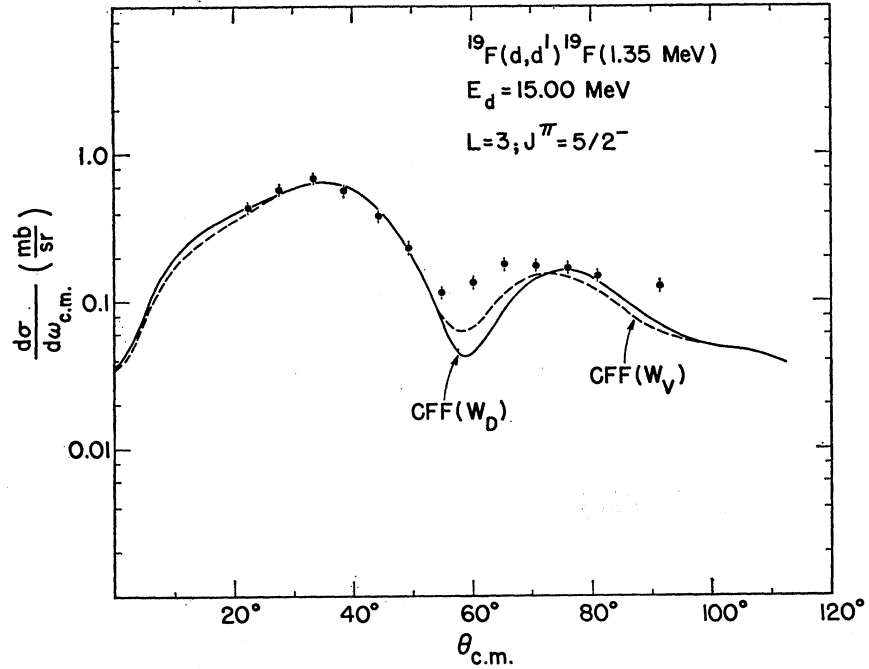


FIG. 5. Differential cross sections of the  $L=3$  transition to the  $J^\pi=5/2^-$  state at 1.35 MeV. Solid line: calculated with  $W_D$ ; broken line: calculated with  $W_V$ .

tion is

$$(d\sigma/d\omega_{J_i \rightarrow J_f}) (\text{expt})$$

$$= [(2J_f+1)/\{(2L+1)(2j_p+1)\}] \beta_L^2 \sigma_{lsj}(\theta), \quad (3)$$

where  $j_p$  is the spin of the particle or hole coupled to a collective vibration or rotation of the adjacent even-even nucleus. Here,  $j_p$  is equal to the spin of the target  $J_i$ . In this model a multiplet of states will be excited with spins between  $L+j_p$  and  $|L-j_p|$ .

Equation (2) applies only to transitions within a rotational band. For Eq. (3) to be valid, the final state must consist of an odd particle in the same orbit as in the target ground state coupled to a rotational or vibrational excitation of the core. If between the initial and final state there is a change of the intrinsic rotational state, or a change in the configuration of the odd particle, the form factors given by the collective prescription are not justified. In the analysis to follow we will assume the strong-coupling rotational model for the  $E2$  excitations and weak particle-core vibrational coupling for the  $E3$  transition.

In the present investigation on F<sup>19</sup> the coefficients  $(J_i L K 0 | J_f K)^2$  and  $(2J_f+1)/\{(2L+1)(2j_p+1)\}$  are accidentally the same because  $j_p=J_i=1/2$ . Therefore, ratios of cross sections cannot be used to discriminate between weak and strong coupling. The  $\beta_L$  values extracted from a distorted-wave (DW) analysis of inelastic scattering may be compared to the reduced electromagnetic transition probability  $B(EL) \downarrow$  using the equation<sup>4,15</sup>

$$B(EL) \downarrow_{L \rightarrow 0} = (9/16\pi^2) [e^2 Z^2 R_e^{2L} \beta_L^2 / (2L+1)], \quad (4)$$

where the downward arrow indicates the deexcitation probability. This relation is based upon the assumption of a uniform spheroidal charge distribution of average radius  $R_e$  and charge  $Z$ . For rotational excitation  $\beta_L$  is simply the deformation parameter of the static deformation. For vibrational nuclei  $\beta_L$  is related to the centroid energy of the vibration  $\hbar\omega_L$  and the surface tension parameter  $C_L$  through the equation

$$\beta_L^2 = (2L+1) (\hbar\omega_L / 2C_L). \quad (5)$$

Introducing the "single-particle unit" or "Weisskopf unit" of the electromagnetic transition probability  $B(EL) \downarrow_{sp}$  as<sup>4</sup>

$$B(EL) \downarrow_{sp} = (1/4\pi) [3/(3+L)]^2 e^2 R_e^{2L} \quad (6)$$

with  $R_e = 1.2 \times A^{1/3}$  F, the transition strength  $|M|^2$  may be defined

$$\begin{aligned} |M|^2 &= B(EL) \downarrow / B(EL) \downarrow_{sp} \\ &= (1/4\pi) [(3+L)^2 / (2L+1)] Z^2 \beta_L^2. \end{aligned} \quad (7)$$

Very often  $|M|^2$  is simply called the  $B(EL) \downarrow$  in single-particle or Weisskopf units (W.u.).

Transition probabilities for excitation  $B(EL) \uparrow$  and deexcitation  $B(EL) \downarrow$  are related through

$$B(EL) \uparrow = [(2J_f+1)/(2J_i+1)] B(EL) \downarrow \quad (8)$$

which for a  $0 \rightarrow L$  transition is

$$B(EL) \uparrow = (2L+1) B(EL) \downarrow. \quad (9)$$

Considerable confusion in the literature has been caused by the fact that some authors include the

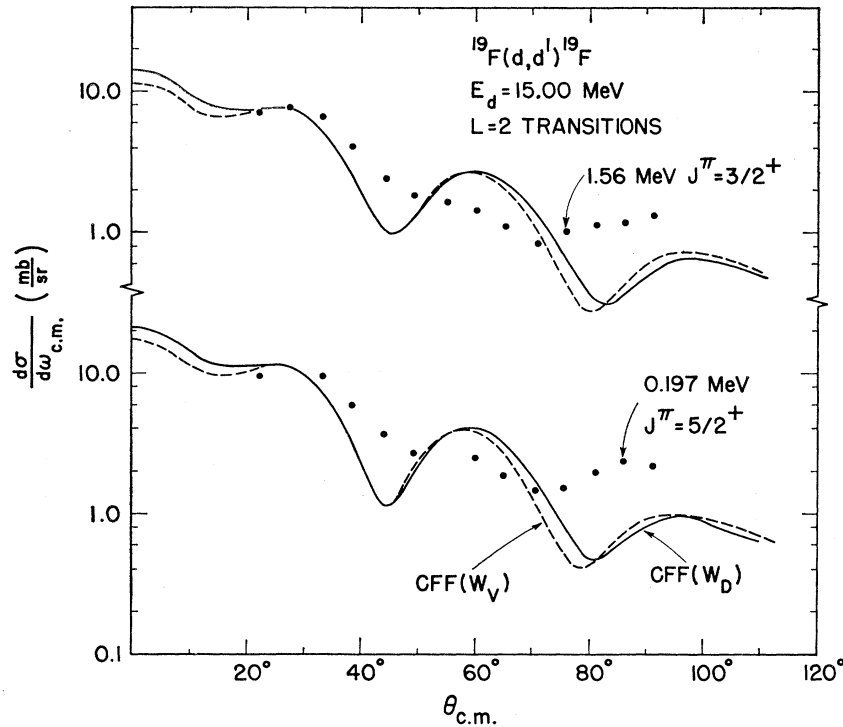


FIG. 6. Differential cross section of  $L=2$  transitions to the  $J^\pi = \frac{3}{2}^+$  state at 0.197 MeV and the  $J^\pi = \frac{5}{2}^+$  state at 1.56 MeV. Solid lines and broken lines as in Fig. 5.

factor  $(2L+1)$  in the definition of the single-particle unit<sup>15</sup> while others do not.<sup>4,16</sup>

It is useful to define the single-particle reduced transition probability for excitation  $B(EL)_{sp} \uparrow$  with the inclusion of the factor of  $(2L+1)$  as done by Alder *et al.*<sup>14</sup> and to omit the factor of  $(2L+1)$  in  $B(EL)_{sp} \downarrow$  as by Wilkinson<sup>16</sup> and Skorka *et al.*<sup>4</sup> Then we have

$$|M|^2 \uparrow = [1/(2L+1)] [(2J_f+1)/(2J_i+1)] |M|^2 \downarrow, \quad (10)$$

which simplifies to  $|M|^2 \uparrow = |M|^2 \downarrow$  for  $0 \rightarrow L$  transitions.

In this paper we will always use the *de*excitation probability  $B(EL) \downarrow$  in units of  $e^2 F^{2L}$  or  $|M|^2 \downarrow$  in Weisskopf units as defined in Ref. 4.

This facilitates comparison with neighboring nuclei. For weakly coupled states in an odd- $A$  nucleus, the  $|M|^2 \downarrow$  will be the same as for the parent collective transition in the adjacent even-even nucleus.

As mentioned in Sec. III, the distorted-wave calculations were performed with two different shapes of the form factor, the derivatives of (a) the optical-model potential with surface absorption and (b) the optical-model potential with volume absorption.

The shapes of the calculated angular distributions were found to be very similar in the two cases, only the absolute cross section was larger by about a factor of 1.5 when the volume absorption term was used. This resulted in a  $\beta_L$  value smaller by a factor of

$\sqrt{1.5}$  compared to the calculations with the usual surface absorption.

As was found in previous complex form factor analyses of inelastic scattering of deuterons<sup>13</sup> and He<sup>3</sup> particles,<sup>17</sup> the calculated absolute cross section is mainly due to the imaginary part of the form factor. For real coupling, we found the cross section to be four times smaller than for complex coupling with a surface term. This effect, however, seems to be less important at higher energies (52-MeV deuterons).<sup>18</sup>

The fit to the  $L=3$  transition to the  $J^\pi = \frac{5}{2}^-$  state is very good (Fig. 5); the calculated  $L=2$  angular distributions, however, show much more oscillatory character than does the experiment (Fig. 6). We have normalized the theoretical curves to the experimental ones at forward angles to extract  $\beta_L$  values. The results are listed in Table II together with values from previous ( $p$ ,  $p'$ ) experiments and from Coulomb excitation.  $B(EL)$  values are listed in Tables III and IV together with theoretical estimates.

Although we estimate the errors in the  $\beta_2^2$  values to be at least 30% in the present experiment (because of the rather poor fits), the agreement with previously published values is amazingly good.

On the other hand, the extracted  $\beta_3$  or  $B(E3)$  values for the  $\frac{5}{2}^- \rightarrow \frac{1}{2}^+$  transition were considerably smaller in the present experiment than in any of the previous investigations.

The strong dependence of  $\beta_L$  on the strength of the

<sup>16</sup> D. H. Wilkinson, in *Nuclear Spectroscopy* (Academic Press Inc., New York, 1960), Part B, p. 852.

<sup>17</sup> E. R. Flynn and Louis Rosen, *Phys. Rev.* **153**, 1228 (1967); E. R. Flynn and R. H. Bassel, *Phys. Rev. Letters* **15**, 168 (1965).

<sup>18</sup> F. Hintenberger, G. Mairle, U. Schmidt-Rohr, G. J. Wagner, and P. Turek, *Nucl. Phys.* **A115**, 570 (1968).

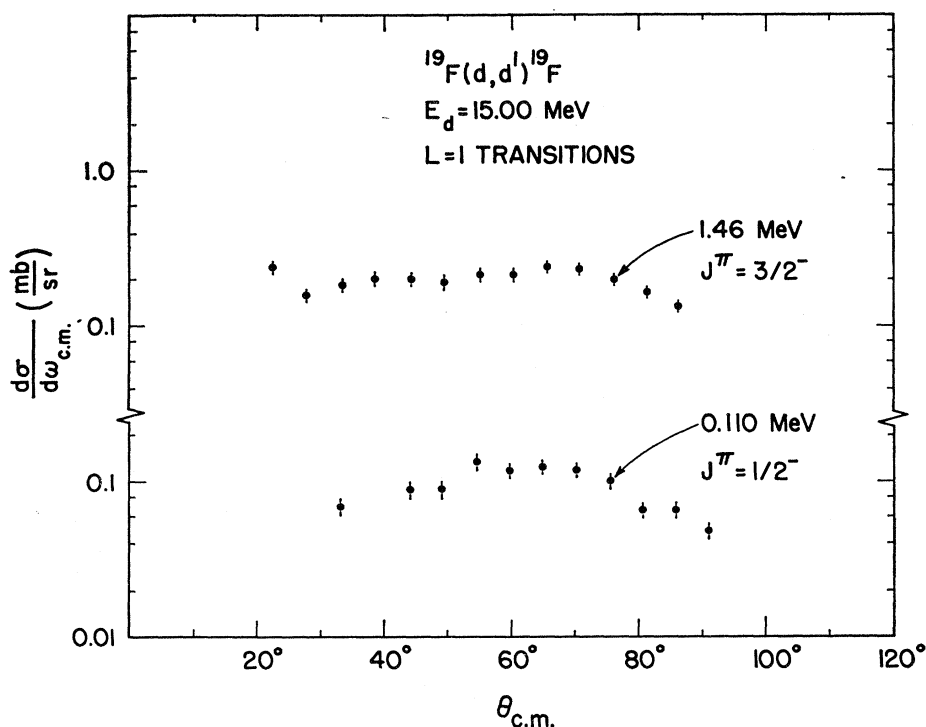


FIG. 7. Differential cross sections of  $L=1$  transitions to the  $J^\pi = \frac{1}{2}^-$  state at 0.110 MeV and the  $J^\pi = \frac{3}{2}^-$  state at 1.46 MeV.

imaginary part of the form factor may cast some doubt on the accuracy of the extracted  $\beta_L$  values. However, the  $\beta_2$  and  $\beta_3$  values are about equally affected by a change in  $W_D$ . Therefore, the ratio of  $\beta_3/\beta_2$  should be fairly reliable. Because the  $\beta_2$  values are in very good agreement with previous results in  $F^{19}$  and neighboring nuclei, we believe the extracted  $\beta_3$  to be correct within about 40%. This puts it far outside the errors given for the two Coulomb-excitation measurements. This discrepancy is not understood. Harvey *et al.*<sup>19</sup> have studied inelastic  $\alpha$  scattering on several nuclei from  $C^{12}$  to  $O^{18}$ . They found good agreement with Coulomb-excitation experiments for the  $B(E2)$  values; however, the  $B(E3)$  values were in general a factor of 2 lower in the  $(\alpha, \alpha')$  experiment. Even if this underestimate of the  $B(E3)$  would be true in general for inelastic-scattering experiments on light nuclei, our  $B(E3)$  would still be considerably lower than the most recent Coulomb-excitation experiment for the  $\frac{5}{2}^-$  to  $\frac{1}{2}^+$  transition.

It is interesting to note that the  $L=1$  transitions to the  $\frac{1}{2}^-$  (0.110-MeV) and  $\frac{3}{2}^-$  (1.46-MeV) levels, although forbidden by all simple models which neglect core excitation,<sup>20,21</sup> are seen in the present experiment. The very small  $B(E1)$  values for these states from Coulomb excitation is evidence for  $5p-2h$  or higher core excitations.<sup>20</sup>

Satchler<sup>22</sup> has suggested a method for treating  $L=1$

transitions within the framework of the collective form factor model. Dipole oscillations of the nuclear shape can be generated, without a center-of-mass shift, by a  $Y_1$  oscillation of the surface thickness  $a$ . However, the angular distributions for the  $L=1$  transitions to the  $\frac{1}{2}^-$  (0.110-MeV) and  $\frac{3}{2}^-$  (1.46-MeV) states (Fig. 7) do not show much structure, so we have not attempted this approach. In contrast, the weak  $L=1$  transitions seen by Harvey *et al.*<sup>19</sup> show a good diffraction pattern.

#### COMPARISON WITH MODEL PREDICTIONS

Various models have been proposed to explain the properties of the low-lying excited levels of  $F^{19}$ . Most of the previous theoretical work has been reviewed in a recent paper by Benson and Flowers.<sup>20</sup> The rotational model<sup>23</sup> provides the simplest description of the low-positive-parity states of  $F^{19}$ . A rotational model based on Nilsson orbit No. 6 with  $K=\frac{1}{2}$  would explain the observed  $J^\pi = \frac{1}{2}^+, \frac{5}{2}^+, \frac{3}{2}^+$  states at 0.0, 0.197, and 1.56 MeV. Calculations by Paul<sup>24</sup> assumed two rotational bands ( $K^\pi = \frac{1}{2}^+$  and  $\frac{3}{2}^+$ ) mixing to explain other states at somewhat higher excitation, but it appears that a single rotational band gives a more satisfactory description of the low-lying states.<sup>20</sup> Also, the shell-model calculation of Elliot and Flowers<sup>25</sup> based on the assumption of three  $2s1d$  particles coupled to an inert  $^{16}O$  core accounts for many of the

<sup>19</sup> B. G. Harvey, J. R. Meriwether, J. Mahoney, A. Bussiere de Nercy, and D. J. Horen, Phys. Rev. **146**, 712 (1966).

<sup>20</sup> H. G. Benson and B. Flowers, Nucl. Phys. **A126**, 305 (1969).

<sup>21</sup> A. Arima, H. Horiuchi, and T. Sebe, Phys. Letters **24B**, 129 (1967).

<sup>22</sup> G. R. Satchler, Nucl. Phys. **A100**, 481 (1967).

<sup>23</sup> S. G. Nilsson, Kgl. Danske Videnskab. Selskab, Mat.-Fys. Medd. **29**, No. 16 (1955).

<sup>24</sup> E. B. Paul, Phil. Mag. **2**, 311 (1957).

<sup>25</sup> J. P. Elliot and B. H. Flowers, Proc. Roy. Soc. (London) **A229**, 536 (1955).

TABLE I. Optical-model parameters for  $F^{10}+d$  at 15.0 MeV.

$V_R$	$r_R$	$a_R$	$W_V$	$4W_D$	$r_I$	$a_I$	$\chi^2$ per point	$\langle r_s^2 \rangle^{1/2}$	$\langle r_t^2 \rangle^{1/2}$
79.6	1.164	0.821	0.0	61.72	1.583	0.613	8.23	3.89	4.89
94.3	1.027	0.806	7.49	0.0	2.175	0.560	8.88	3.67	4.95

TABLE II.  $\beta_L$  values from CFF analysis.

$E_x$	$J_{\text{final}}^\pi$	$L$	$\beta_L$ ( $p, p'$ ) (17 MeV) real CFF <sup>a</sup>	$\beta_L$ present experiment ( $d, d'$ ) Complex CFF surface abs.	Complex CFF volume abs.	$\beta_L$ Coulomb excitation
0.197	$\frac{5}{2}^+$	2	0.49±0.02	0.53±0.08	0.43±0.06	0.46 <sup>b</sup>
1.56	$\frac{3}{2}^+$	2	0.51±0.02	0.56±0.09	0.47±0.07	0.45 <sup>c</sup>
1.35	$\frac{5}{2}^-$	3	0.35±0.04	0.21±0.04	0.17±0.04	0.62 <sup>b</sup> 0.49 <sup>c</sup>

<sup>a</sup> Reference 2.<sup>b</sup> Reference 3.<sup>c</sup> Reference 5.TABLE III.  $B(E2)$ 's and transition strengths  $|M|^2 \downarrow$  of observed  $L=2$  transitions.

	$B(E2) \downarrow_{1/2_+^{5/2+}}$ ( $e^2 F^4$ )	$B(E2) \downarrow_{1/2_+^{3/2+}}$ ( $e^2 F^4$ )	$ M ^2 \downarrow_{1/2_+^{5/2+}}$	$ M ^2 \downarrow_{1/2_+^{3/2+}}$	Reference
Coulomb exc.	21	21	7±2	6.8±0.7	3, 5
( $p, p'$ )	24	26	8±0.7	9±0.7	2
( $d, d'$ ) <sub>WV</sub>	23	25	7.7±2	8.5±3	This experiment
( $d, d'$ ) <sub>WD</sub>	27	30	9±3	10±3	This experiment
Intermediate-coupling model	24	21.5	8	7.2	19

TABLE IV.  $B(E3) \downarrow$  values and  $|M|^2 \downarrow$  transition strengths of  $\frac{5}{2}^- (1.35) \rightarrow \frac{1}{2}^+$  (g.s.) transition.

	$B(E3) \downarrow$ ( $e^2 F^6$ )	$ M ^2 \downarrow_{E3}$	$e_{\text{off}}$	Reference
Nilsson model	4.3	0.2	...	21, 23
Weak coupling	65	3.0	1.0 <sup>a</sup>	21
$SU_3$ shell model	38	1.76	1.1 <sup>b</sup>	26
	22	1.0	0.61 <sup>c</sup>	26
Intermediate-coupling model	216	10.0	2.0 <sup>d</sup>	20
	164	7.6	1.6 <sup>e</sup>	20
Coulomb excitation	260	12.0±4.0	...	3
Coulomb excitation	164	7.6±1.3	...	5
( $p, p'$ ) at 17.5 MeV	82	≤3.8±0.6	...	2
( $d, d'$ ) present experiment ( $W_D$ )	32	1.4±0.6	...	...
( $d, d'$ ) present experiment ( $W_V$ )	21	0.9±0.5	...	...

<sup>a</sup> Not clearly defined in Ref. 21.<sup>b</sup> Effective charge necessary to explain earlier value of the  $3^- \rightarrow 0^+$  transition strength in  $O^{16}$ .<sup>c</sup> Effective charge adjusted to fit  $B(E3)$  for  $O^{16}$  of Ref. 27.<sup>d</sup> Large value used to reproduce early<sup>19</sup> Coulomb-excitation result.<sup>e</sup> Effective charge to fit Coulomb-excitation value of Ref. 5.

observed properties of  $F^{19}$ . Benson and Flowers<sup>20</sup> performed a full intermediate-coupling calculation similar to the calculations of Elliot and Flowers but with a different residual interaction and reproduced the  $B(E2)$  values for the positive-parity states with a reasonable value for the effective charge (Table III). In any case, the predictions of the various models for the positive-parity states differ significantly only for the states above 3 MeV, which were not covered by the present investigation.

The negative-parity states may be obtained<sup>21</sup> by weakly coupling a  $1p_{1/2}$  proton hole to the ground-state  $K^\pi=0^+$  rotational band in  $Ne^{20}$ . In the strong-coupling model we may assume a  $K^\pi=\frac{1}{2}^-$  rotational band based on Nilsson orbit No. 4. Harvey<sup>26</sup> applied the  $SU_3$  shell model to explain the properties of the negative-parity states and fitted the  $E2$  transition strengths quite well for the transitions between the negative-parity states. The major difficulty for any model has been the previously observed large  $B(E3)$  value of the  $\frac{5}{2}^- \rightarrow \frac{1}{2}^+$  transition (Table IV). The comparison between the various model predictions for the  $E3$  transition is difficult, because in some calculations harmonic-oscillator wave functions were used, in others wave functions based on a Woods-Saxon potential. This results in quite different effective charges  $e_{\text{eff}}$  for the same configurations. Furthermore, some authors adjust  $e_{\text{eff}}$  to fit the  $B(E3)$  in  $F^{19}$  while others fix  $e_{\text{eff}}$  by fitting  $E3$  transitions in neighboring nuclei such as  $O^{16}$ .

In the  $SU_3$  calculation of Harvey<sup>26</sup> an  $e_{\text{eff}}=1.1$  was chosen to fit an early value (29 W.u.) of the  $B(E3)$  for the  $3_1^- \rightarrow 0_1^+$  transition in  $O^{16}$ . The new value<sup>27</sup> for  $O^{16}$  of 14 W.u. would require an  $e_{\text{eff}}$  of 0.61. This lower value would then give  $|M|^2 \downarrow = 1.0$  for the  $\frac{5}{2}^- (1.35) \rightarrow \frac{1}{2}^+ (\text{g.s.})$   $B(E3)$  in  $F^{19}$ , in good agreement with our value but much lower than the Coulomb-excitation result. We have scaled the  $B(E3)$  as  $(1+2e_{\text{eff}})^2$  for  $O^{16}$  and as  $(1+e_{\text{eff}})^2$  for  $F^{19}$  where only the protons are involved in the transition.

Benson and Flowers<sup>20</sup> in their intermediate-coupling calculation, find an isoscalar effective charge of 0.25 (with Woods-Saxon orbitals) is necessary to explain the  $B(E2)$  transition in  $F^{19}$ , while an effective charge of 2 would be needed to explain the early  $B(E3)$  strength (Table IV) of  $|M|^2 \approx 10$  W.u.

Our experimental value of 1.4 W.u. would imply  $e_{\text{eff}}=0.12$  in the Benson and Flowers calculations, while the new Coulomb-excitation value of 7.6 W.u. requires  $e_{\text{eff}}=1.6$ . Again we have scaled the  $B(E3)$  as  $(1+e_{\text{eff}})^2$ .

It thus appears that most current models cannot explain a  $B(E3)$  as large as 7.6 W.u. without large effective charges.

Large  $B(E3)$ 's between the lowest  $K=\frac{1}{2}^+$  and  $K=\frac{1}{2}^-$  bands can be obtained if  $F^{19}$  is assumed to possess a static octupole deformation or be very soft for octupole vibrations. Krappe and Wille<sup>28</sup> apply the Bohr-Mottelson unified model to  $F^{19}$ , assuming static quadrupole and octupole deformations and include rotation-vibration coupling. They are able to explain the large  $B(E3)$  (7.6 W.u.), most of the  $B(E2)$ 's, and the level spacings within the  $K=\frac{1}{2}^+$  and  $K=\frac{1}{2}^-$  bands with deformation parameters,  $\delta=0.4$  (quadrupole) and  $a_3=0.14$  (octupole). However, they need a moment-of-inertia parameter  $\mathcal{J}$  three times smaller than that for  $Ne^{20}$ , and an anomalously large  $B$  (measuring increase of  $\mathcal{J}$  with angular momentum). Moreover, the zero-point amplitude of the octupole vibration which they find is larger than the static deformation which they assume to fit the  $B(E3)$ . This raises questions concerning the validity of the calculation.

Finally, a point should be made regarding the validity of using collective form factors in the DWBA to extract " $B(EL)$ " values for transitions which are not strongly collective or when single-particle as well as shape excitations are involved.

If the 1.35-MeV,  $J^\pi=\frac{5}{2}^-$  state is a member of the  $\frac{5}{2}^-$ ,  $\frac{7}{2}^-$  weak coupling doublet based on the collective octupole vibration which is seen in  $Ne^{20}$  at 5.62 MeV, then the DWBA analysis with CFF should be valid and there is a serious discrepancy between our results and the Coulomb-excitation measurements. On the other hand, if the  $\frac{1}{2}^+$  and  $\frac{5}{2}^-$  (1.35-MeV) states are members of  $K=\frac{1}{2}^+$  and  $K=\frac{1}{2}^-$  rotational bands,<sup>23</sup> or, as suggested by Arima,<sup>21</sup>  $2s_{1/2}$  and  $1p_{1/2}$  proton holes in the  $Ne^{20}$  ground and  $2+$  excited states, respectively, then the use of CFF's is not expected to be correct. For either of these latter pictures, a single hole excitation (from  $K=\frac{1}{2}^+$  to  $K=\frac{1}{2}^-$  or, alternatively, from  $2s_{1/2}$  to  $1p_{1/2}$ ) and a collective  $E2$  excitation (within the  $K=\frac{1}{2}^-$  or  $K=\frac{1}{2}^+$  bands, or of the  $Ne^{20}$  core) is required to excite the  $\frac{5}{2}^-$  state. In this case the actual form factor will be different than that given by a  $Y_3$  deformation of the surface as in the usual CFF prescription for an  $E3$  transition. The same is true for the  $SU_3$ <sup>26</sup> and intermediate-coupling<sup>20</sup> models where a change in the particle state is involved in an  $E3$  excitation. It is then not surprising that quite different  $B(E3)$ 's are obtained from Coulomb excitation, inelastic proton, and inelastic deuteron scattering. Calculations with realistic microscopic form factors are needed to harmonize the various experimental results.

#### ACKNOWLEDGMENT

The authors are indebted to Dr. B. Bayman for helpful discussions.

<sup>26</sup> M. Harvey, Nucl. Phys. 52, 542 (1964).

<sup>27</sup> T. K. Alexander and K. W. Allen, Can. J. Phys. 43, 1563 (1965).

<sup>28</sup> H. J. Krappe and U. Wille, Nucl. Phys. A124, 641 (1969), and references therein.